[AMERICAN JOURNAL OF SCIENCE, VOL. 277, JUNE, 1977, P. 735-749]

# STABILITY RELATIONS OF GRUNERITE, $Fe_7Si_8O_{22}(OH)_2$

WARREN C. FORBES

Department of Geological Sciences,
University of Illinois, Chicago Circle, Chicago, Illinois 60680

ABSTRACT. The stability limits of grunerite, a major constituent of metamorphosed iron formations, are:

| P,kb | HM | NNO | QFM | WM |
|---|---|---|---|---|
| 1 | 560±15 | 665±15 | 685±15 | 630±10 |
| 2 | 570±15 | 670±15 | 690±15 | 635±10 |
| 3 | 585±15 | 685±15 | — | 640±10 |

The enhanced thermal stability at intermediate oxygen fugacities may be due to the presence of ferric ions which reduce strain between the octahedral and tetrahedral layers arising from the inherent misfit of these units. Indices of refraction and the angle of extinction increase with increasing oxygen fugacity. X-ray data on a completely dehydrogenated grunerite are presented.

## INTRODUCTION

The metamorphism of iron formations generally involves devolatilization reactions through which the original carbonate and phyllosilicate minerals are converted to amphiboles, pyroxenes, and olivines. An important aspect to our understanding of this metamorphism has been the determination of the physical parameters of temperature, pressure, and vapor compositions existing during the metamorphic event. To this end, the thermal stability limits of several important constituent minerals have been investigated to provide information bearing on this problem.

Grunerite [$Fe_7Si_8O_{22}(OH)_2$] is a major constituent of moderately metamorphosed iron formations and has been used as an index to metamorphic grade by French (1968). Its appearance generally coincides with the biotite isograd, present in adjacent rocks (James, 1955), and its breakdown occurs under conditions of the sillimanite zone. Thus data on the stability of this mineral can yield considerable information on the T, P, and $fo_2$ conditions prevailing during metamorphism.

## PREVIOUS WORK

Grunerite is a difficult mineral to synthesize directly from oxide starting materials. Flaschen and Osborn (1957) found that grunerite formed only as a metastable decomposition product of minnesotaite [$Fe_3Si_4O_{10}(OH)_2$] at temperatures greater than 480°C and concluded that grunerite did not have a stability range under the conditions investigated. Smith (1957) and Forbes (1971a) attempted to duplicate the experiments of Flaschen and Osborn but were unsuccessful.

Kopp and Harris (1967) synthesized grunerite in the system NaO–Fe–$SiO_2$–$H_2O$, and Schürmann (1967) produced the amphibole by using grunerite bulk compositions to which 2.7 wt percent CaO had been added. However, in each of the above cases, the chemical composition of the amphibole produced may depart significantly from the ideal $Fe_7Si_8O_{22}(OH)_2$ formula. Forbes (1971b) was able to synthesize grunerite by using

extremely fine grained hematite (1-5$\mu$m) and quartz (3-6$\mu$m) plus excess water. The maximum yield of amphibole was about 5 to 10 percent, and this decreased markedly at oxygen fugacities above those defined by the magnetite–wüstite buffer (Eugster, 1957).

## EXPERIMENTAL METHOD

Experiments were made using standard hydrothermal techniques. Cold-seal vessels (Tuttle, 1949) were heated in vertical, nichrome-wound furnaces, controlled by Barber-Coleman power proportioning regulators. Temperatures were measured by chromel-alumel thermocouples, periodically calibrated against the melting point of NaCl (800.5°C). Temperature variations were between 2° and 6°C, and temperatures reported are the means of the observed variations. Pressure to the vessels was measured by a Heise gauge, and fluctuations were less than ±50 bars.

Oxygen fugacities were buffered using the technique of Eugster (1957) and the data of Huebner and Sato (1970) and Wones and Gilbert (1969). The hematite-magnetite (HM), nickel-nickel oxide (NNO), quartz-fayalite-magnetite (QFM), and magnetite-iron—magnetite-wüstite (MI—MW) buffer series were employed. Platinum capsules were used throughout the study. At the temperatures involved in this work (<750°C), iron loss to the capsule was considered negligible.

In view of the low yields of grunerite produced in direct synthesis runs, starting material seeded with natural grunerite was used for the majority of runs. Approximately 1.5 wt percent of grunerite was added to finely ground hematite and quartz, weighed out in the requisite proportions. The grunerite was from the Labrador Trough (Mueller, 1960) and was kindly supplied by Dr. E. Olsen, Field Museum of Natural History. The analysis of this material is as follows: $SiO_2$, 48.48; $Al_2O_3$, 1.19; $Fe_2O_3$, 2.40; FeO, 42.05; MnO, 2.80; MgO, 1.93; $Na_2O$, 0.12; $H_2O+$, 1.58. Calcium is less than 0.1 percent. This is a very iron-rich grunerite, and the effects of MgO+MnO on the overall composition of the starting material are minimal.

Using seeded starting material, reaction directions were indicated by changes in the amount of grunerite present within the run. After grinding, run charges were examined optically and compared to a photomicrograph of the starting material in roughly the same amount and degree of dispersion. Within the stability field of grunerite and using either the MI or QFM buffer, the percentage of the amphibole increased to about 10 percent of the condensed assemblage. At the relatively higher oxygen fugacities, increases in the amount of grunerite were much less, and often no growth was apparent.

The decomposition rate of grunerite is also dependent on oxygen fugacity. Run durations of less than 7 days were needed on the MW buffer to note clearly a reduction in the amount of grunerite present. Runs of up to 3 weeks duration were required to establish run direction on the NNO and HM buffers. Even in these long term runs, traces of grunerite were often present.

Direct synthesis runs, using hematite and quartz as a starting material, were successful on all but the HM buffer. Yields were greatest at low oxygen fugacities.

Standard optical and power X-ray diffraction techniques were used to identify and characterize the phases produced in the synthesis runs. In the majority of runs, the amount of grunerite present was too low to be detected by X-ray diffraction; in these runs, optical examination sufficed.

## RESULTS

The stability relations of grunerite were examined at temperatures ranging from 425° to 725°C and at pressures from 500 to 3000 bars $P_{H_2O}$. Oxygen fugacities were defined by the MI–MW, QFM, NNO, and HM buffer series. The equilibrium diagrams are presented in figures 1 to 4. Pertinent synthesis and reversal data relating to the positions of the decomposition curves are given in table 1.

The grunerite decomposition curve at oxygen fugacities defined by the MW buffer is shown in figure 1. This curve marks the dehydration of grunerite to fayalite plus quartz plus vapor. This reaction occurs at 640 ± 10°C and 3000 bars, 635 ± 10°C and 2000 bars, and 630 ± 10°C at 1000 bars. Reaction reversals were accomplished at 1000 and 2000 bars using finely ground fayalite and quartz, with excess water as starting material. Rosettes of accicular grunerite crystals were produced in runs of 3 days' duration generally with a yield of less than 1 percent. As with all buffer series, the initial position of the decomposition curve was based on both direct synthesis runs and by changes in the amount of grunerite in the seeded runs. On the high temperature side of the curve, grunerite disappeared from the condensed assemblage in runs of approximately 7 days' duration.

The maximum thermal stability limit for grunerite was found at oxygen fugacities defined by the QFM buffer (fig. 2). Grunerite reacts with gas to form the assemblage magnetite plus fayalite plus quartz plus vapor at 695 ± 10°C and 2000 bars and 685 ± 10°C at 1000 bars. The reaction was reversed at 1000 bars by placing the assemblage fayalite–magnetite–quartz–water at 675°C for 2 weeks. The yield of grunerite was extremely small. On the high temperature side of the curve, grunerite within the seeded runs is encrusted with fayalite in runs of 5 days' duration. The amphibole completely disappears in runs of 12 days' time.

The reaction of grunerite with vapor at oxygen fugacities defined by the NNO buffer to magnetite, quartz, and vapor occurs at 660 ± 10°C at 1000 bars and 675 ± 10°C at 2000 bars. The position of the curve is based on the data from runs using seeded starting materials, as reversal runs were not successful (table 1). Runs of up to 21 days' duration were required to establish unequivocably the growth or decay of grunerite. Grunerite persists metastably at temperatures 75°C above the breakdown curve in runs of 5 to 7 days' duration. In direct synthesis runs, the maximum yield of grunerite is less than 1 percent. At 1000 bars, the stability

TABLE 1

| Temp. °C | Pressure, kb | Time, days | Run products |
|---|---|---|---|
| | Hematite–magnetite buffer | | |
| 535 | 1 | 10 | Q+H+Gr+M? |
| 550 | 1 | 14 | $\overline{Q}$+$\overline{H}$+Gr+$\overline{M}$? |
| 565 | 1 | 22 | $\overline{Q}$+$\overline{H}$+M+$\underline{Gr}$? |
| 579 | 1 | 3 | Q+H+$\underline{Gr}$ |
| 585 | 1 | 10 | Q+H+$\overline{M}$ |
| 550 | 2 | 22 | Q+M+Gr+H? |
| 565 | 2 | 7 | $\overline{Q}$+$\overline{H}$+Gr+$\overline{M}$ |
| 580 | 2 | 3 | $\overline{Q}$+$\overline{M}$+H+$\underline{Gr}$ |
| 585 | 2 | 21 | Q+M+H |
| 570 | 3 | 2 | Q+H+Gr |
| 580 | 3 | 5 | $\overline{Q}$+$\overline{H}$+Gr |
| 590 | 3 | 22 | $\overline{Q}$+$\overline{M}$+H |
| | Nickel–nickel oxide buffer | | |
| 637 | 1 | 8 | Q+M+Gr |
| 645 | 1 | 12 | $\overline{Q}$+$\overline{M}$+Gr |
| 660 | 1 | 22 | $\overline{Q}$+$\overline{M}$+Gr |
| 668 | 1 | 22 | $\overline{Q}$+$\overline{M}$ |
| 670 | 1 | 11 | Q+M+$\underline{Gr}$ |
| 680 | 1.5 | 17 | Q+M |
| 645 | 2 | 30 | Q+M+Gr |
| 665 | 2 | 4 | $\overline{Q}$+$\overline{M}$+Gr+ |
| 678 | 2 | 21 | $\overline{Q}$+$\overline{M}$ |
| 680 | 2 | 57 | Q+M+Gr* |
| 757 | 2 | 5 | Q+M+$\overline{Gr}$ |
| 650 | 3 | 3 | Q+M+$\overline{Gr}$ |
| 670 | 3 | 5 | $\overline{Q}$+$\overline{M}$+Gr |
| 683 | 3 | 25 | $\overline{Q}$+$\overline{M}$+Gr |
| 690 | 3 | 7 | $\overline{Q}$+$\overline{M}$+$\underline{Gr}$ |

* Starting material = Q+Fa.
** Starting material = natural grunerite.
*** Starting material = Q+F+M.

limit of grunerite on the NNO buffer is about 25°C lower than the maximum limit shown on the QFM buffer and is some 30°C higher than the stability limit defined on the MW buffer (fig. 3).

The decomposition temperature of grunerite is further depressed at oxygen fugacities represented by the HM buffer (fig. 4). The dehydration curve of the amphibole for this buffer series is placed at 570 ± 15°C at 2000 bars and 560 ± 20°C at 1000 bars. The large uncertainty limits are attributed to the "zone of indifference" (Boyd, 1959) marking very sluggish reaction rates. At these relatively high oxygen fugacities, reversal and direct synthesis runs were not successful, and the decision regarding growth or decay of the seed material was especially subjective near the decomposition curve.

Pertinent run data for the stability limits of grunerite

| Temp. °C | Pressure, kb | Time, days | Run products |
|---|---|---|---|
| | Quartz–fayalite–magnetite buffer | | |
| 672 | 1 | 8 | Q+M+F+Gr |
| 675 | 1 | 5 | $\underline{Q}$+$\underline{M}$+$\underline{Gr}$+F? |
| 675 | 1 | 14 | $\underline{Q}$+$\underline{F}$+M+$\underline{Gr}$** |
| 680 | 1 | 7 | $\underline{Q}$+$\underline{F}$+$\underline{M}$+$\underline{Gr}$ |
| 690 | 1 | 3 | $\underline{Q}$+$\underline{F}$+$\underline{M}$+Gr |
| 700 | 1 | 5 | Q+F+M+$\underline{Gr}$? |
| 703 | 1 | 12 | Q+F+M |
| 680 | 2 | 7 | $\underline{Q}$+M+Gr |
| 690 | 2 | 6 | $\underline{Q}$+$\underline{M}$+F+Gr |
| 700 | 2 | 5 | $\underline{Q}$+$\underline{M}$+$\underline{F}$ |
| 690 | 2.75 | 12 | Q+M+F+Gr |
| 705 | 3 | 7 | $\underline{Q}$+$\underline{F}$+$\underline{M}$ |
| | Magnetite–iron—magnetite–wüstite buffer | | |
| 610 | 1 | 11 | $\underline{Q}$+F+Gr |
| 620 | 1 | 4 | $\underline{Q}$+$\underline{F}$+Gr |
| 630 | 1 | 11 | $\underline{Q}$+$\underline{F}$+Gr |
| 630 | 1 | 3 | Q+F+Gr* |
| 640 | 1 | 8 | Q+F |
| 650 | 1 | 10 | Q+F* |
| 620 | 2 | 14 | $\underline{Q}$+F+Gr* |
| 625 | 2 | 10 | $\underline{Q}$+$\underline{F}$+Gr |
| 638 | 2 | 14 | $\underline{Q}$+$\underline{F}$ |
| 640 | 2.6 | 10 | Q+F |
| 620 | 3 | 15 | $\underline{Q}$+F+Gr |
| 630 | 3 | 4 | $\underline{Q}$+$\underline{F}$+Gr |
| 640 | 3 | 7 | $\underline{Q}$+$\underline{F}$ |
| 650 | 3 | 6 | Q+F+$\underline{M}$+$\underline{Gr}$** |

Abbreviations: Q = quartz; F = fayalite; Gr = grunerite; M = magnetite; H = hematite. Vapor is present in all assemblages. Phases underlined are believed to be metastable. Starting material was hematite and quartz, seeded with grunerite where noted. Phases are listed in order of abundance.

The stability field of grunerite as a function of oxygen fugacity and temperature at 1000 bars total pressure is shown in figure 5. Comparable figures at higher pressures would be shifted to only slightly higher temperatures, as the increase in stability with pressure as indicated in figures 1 to 4 ranges from 5° to 10°C per 1000 bars total pressure.

The invariant point G on figure 5 representing the coexistence of five phases in the four component system marks the maximum thermal stability limit of grunerite at this pressure. At higher or lower oxygen fugacities, this limit decreases sharply. The stability region of grunerite is bounded by the assemblages: hematite–quartz–vapor; magnetite–quartz–vapor; fayalite–quartz–vapor, with the nature of the assemblage being determined by oxygen fugacity. An additional invariant point is shown as point H and marks the coexistence of grunerite–hematite–magnetite–quartz and vapor.

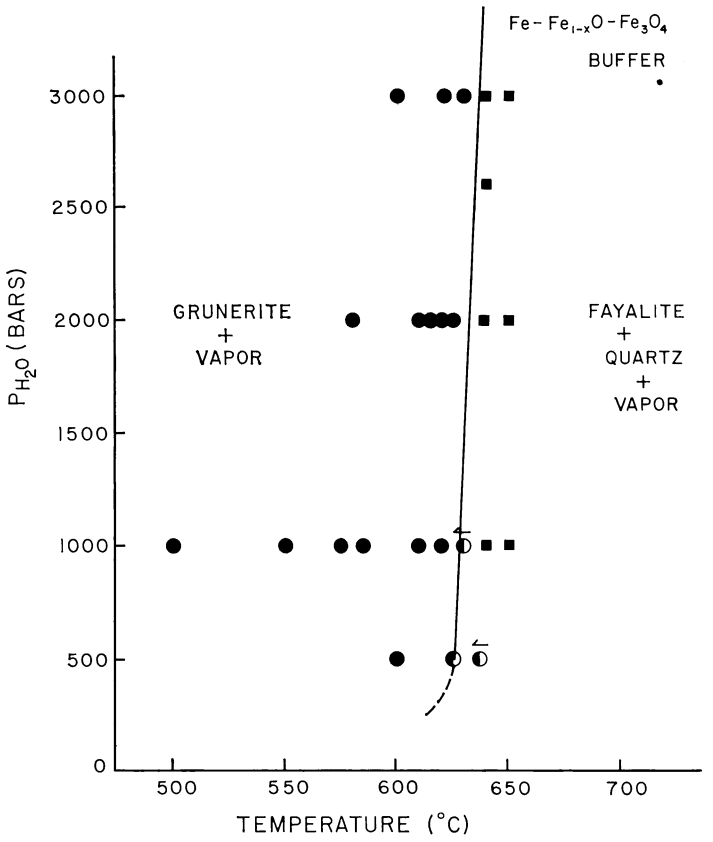


Fig. 1. Pressure-temperature diagram of the stability limits of grunerite plus excess vapor under oxygen fugacities defined by the *magnetite–wüstite* buffer. Filled circles indicate the growth of grunerite; squares indicate the absence of grunerite; partially filled circles indicate the presence of both high and low temperature phases.

Schreinemacher's treatment of the equilibria indicates that an additional reaction governs the stability of grunerite. This reaction: grunerite + magnetite = fayalite + $O_2$ + $H_2O$ would be important in silica-free environments.

## PROPERTIES OF GRUNERITE

Refractive indices of grunerite equilibrated at oxygen fugacities represented by the several buffer series are listed in table 2. All values listed represent measurements taken on at least a dozen grains per run and averaged for approx 10 runs on each buffer series. Changes in refractive indices are small but finite. The indices increase with relatively higher oxygen fugacities. A significant increase in extinction angle was also noted. The variation in Z$\wedge$C of 11° to 20° is equivalent in magnitude to the variation in extinction found by Klein (1964) in the cumming-

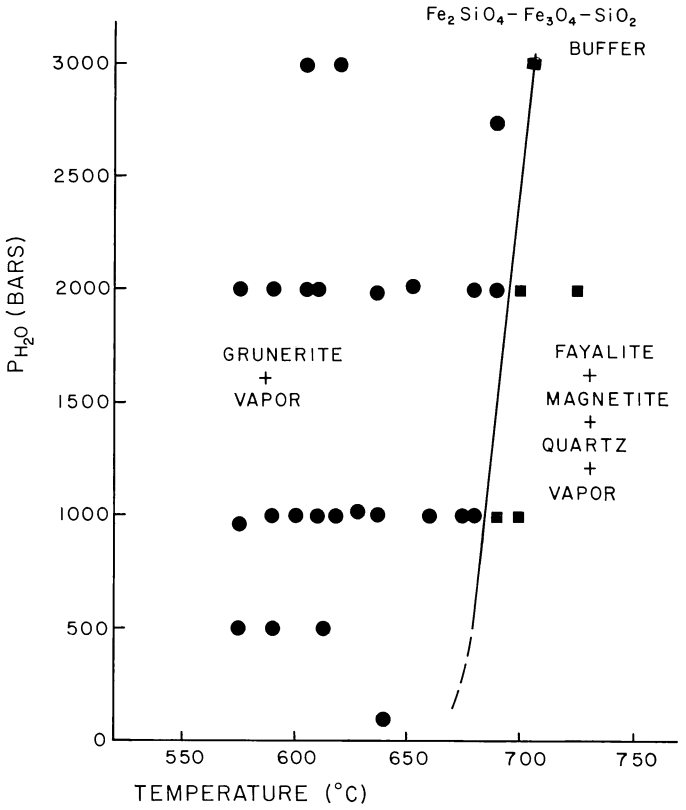


Fig. 2. Pressure-temperature diagram: *quartz–fayalite–magnetite* buffer. Symbols as in figure 1.

tonite–grunerite series over the compositional range 60 to 100 mol percent $Fe_7Si_8O_{22}(OH)_2$. Klein suggested that variations in $\gamma$ and $Z\wedge C$ could be used to determine the magnesium content of grunerite. The data shown in table 2 indicate that this suggestion be used with caution.

Several large (1 × 0.2 mm) crystals were oxidized in air at 585°C. After 18 hours, the crystals were marked by a dark brown shell, surrounding unoxidized amphibole in the center. The junction between oxidized and unoxidized material is sharp and appears to be a cleavage surface. A temperature of 700°C was required for complete oxygenation. This oxidized material was annealed at oxygen fugacities of the HM, NNO, QFM, and MI–MW buffers and at temperatures within the stability field of grunerite. In runs of 4 to 7 days duration, the oxidized material assumed the optical properties shown in table 2, demonstrating the reversibility of the oxidation process.

## X-RAY PARAMETERS

X-ray powder data for grunerite annealed on the MW buffer and completely oxidized grunerite are presented in table 3. The unit cell

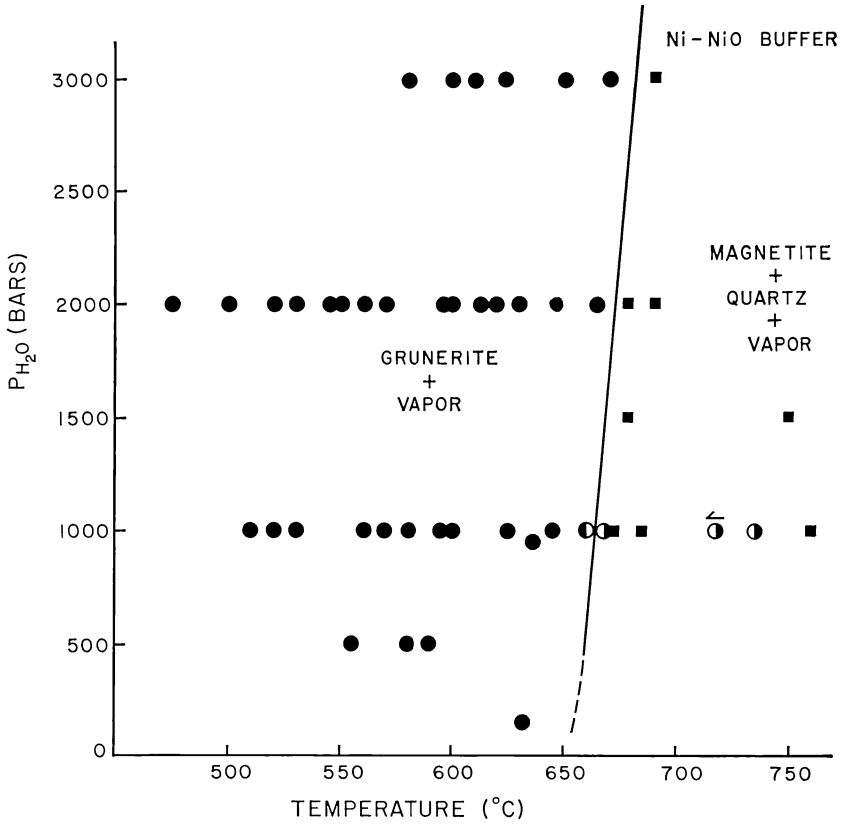


Fig. 3. Pressure-temperature diagram: *nickel–nickel oxide* buffer. Symbols as in figure 1.

parameters were determined by using the program of Evans, Appleman, and Handwerker (1963). From 10 to 14 reflections were calibrated against nearby peaks of Lake Toxaway quartz which was used as an internal standard. The parameters of the annealed grunerite are in agreement with those presented by Finger (1969).

Variations in optical and X-ray properties with oxygen fugacity are similar to those in other hydrous iron silicates reported by Eugster and Wones (1962), Wones (1963), Ernst (1962, 1968), Gilbert (1966), and Semet (1973) and are attributed to the dehydrogenation of grunerite following the reaction:

$$Fe^{+2}_{7}Si_8O_{22}(OH)_2 \rightleftarrows Fe^{+2}_{5}Fe^{+3}_{2}Si_8O_{24} + H_2$$

Oxidation of grunerite results in a decrease of the unit cell parameters, producing a 4 percent reduction in the cell volume. Shrinkage of the *a* and *b* parameters is due to the replacement of two ferrous ions by the smaller ferric ion with the concomitant loss of hydrogen. The small reduction in cell volume and the relative ease with which oxidized

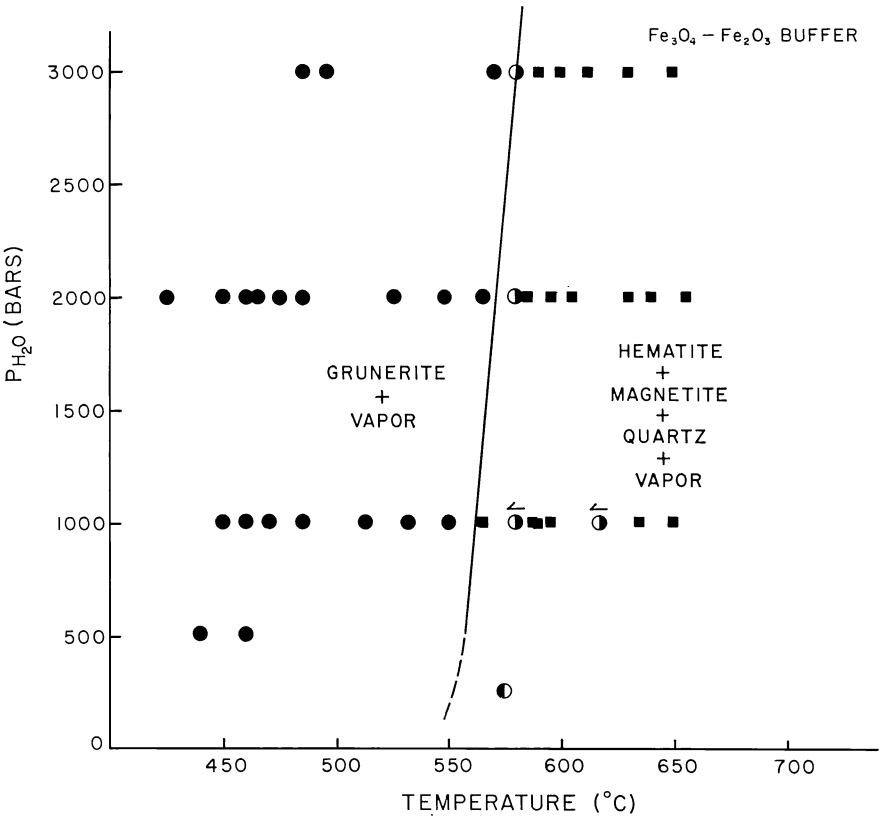


Fig. 4. Pressure-temperature diagram: *hematite–magnetite* buffer. Symbols as in figure 1.

grunerite can be rehydrogenated suggest that complex reduction-substitutions such as $Fe^{+3} + H \rightleftarrows Si^{+4}$ (Forbes, 1969, 1972) do not occur in grunerite.

## DISCUSSION

The shape of the $fo_2$–T stability region of grunerite differs from those of other hydrous ferroan silicates in that the maximum stability temperature occurs at an intermediate oxygen fugacity value (see Eugster and Wones, 1962; Gilbert, 1966). There are several possible explanations for this behavior. Eugster and Wones (1962) found that in the presence of excess quartz, the stability region of annite diminishes, and the point of maximum thermal stability shifts from the MW buffer to the QFM buffer. In the case of grunerite, "excess quartz" is present as the starting materials never gave 100 percent yields of grunerite. However the decomposition assemblages of grunerite are insensitive to the amounts of quartz present in contrast to those of annite. Thus the presence of free quartz should have no effect on the stability of grunerite.

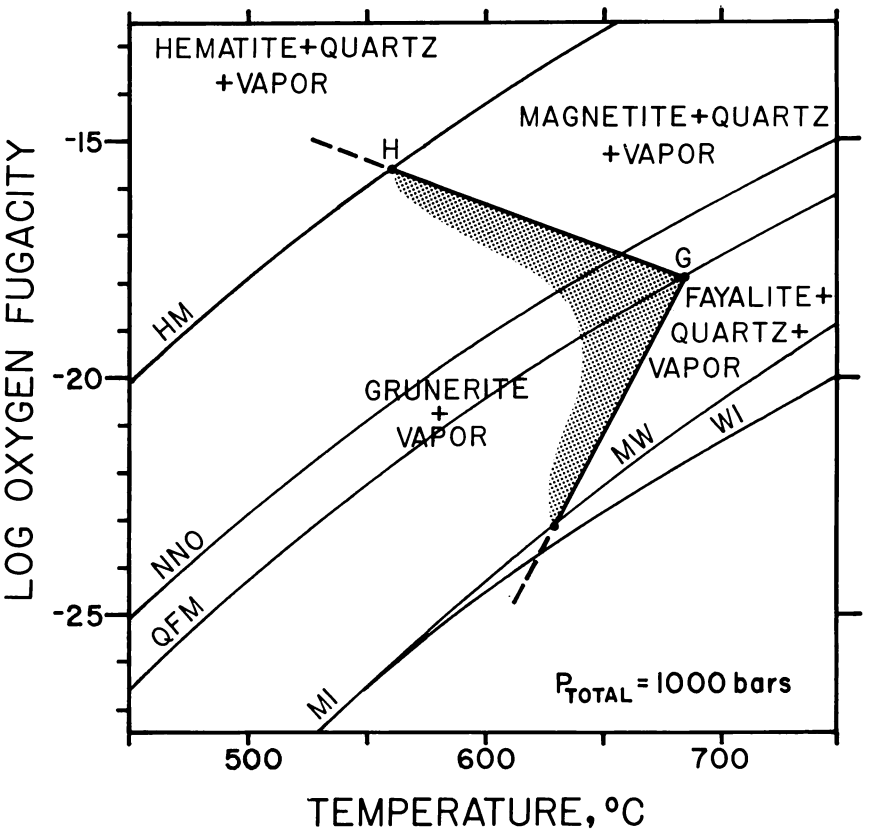


Fig. 5. Stability limits of grunerite on the $fo_2$–T plane at 1000 bars pressure.

TABLE 2

Optical properties of grunerite

| Buffer series | $n_\alpha$ | $n_\gamma$ | Z∧c |
|---|---|---|---|
| HM | 1.690(2) | 1.725(3) | 20° |
| NNO | 1.688(2) | 1.722(3) | 17° |
| QFM | 1.686(2) | 1.722(2) | 13° |
| MI-MW | 1.684(2) | 1.720(2) | 11° |
| Seed Material | 1.684(2) | 1.719(2) | 10-11° |
| Air* | 1.787 | — | parallel extinction |

* Natural grunerite oxidized in air at 585°C—48 hrs; 700°C— 2hrs.

Alternatively, figure 5 suggests that the thermal stability of grunerite is enhanced by the presence of ferric iron within the structure. At oxygen fugacities defined by the QFM buffer, it is probable that a finite oxygrunerite component is present. As shown by Wones (1963) and Charles (1974), progressive $Fe^{+2}$ for Mg substitution in biotites and amphiboles produces a flattening of the octahedral layer, with an increase in the *b* dimension. The tetrahedra within the sheets (biotites) or chains (amphiboles) must rotate about *a* to maintain articulation with the octahedral layer. This produces a kinking in the chain and is a common feature in amphiboles. The degree of tetrahedral rotation is particularly marked in grunerite, which has the largest rotation of eight monoclinic amphiboles examined by Papike, Ross and Clark (1969). The average T–O–T angle is 142.8° for grunerite with a Fe/(Fe+Mg) ratio of 0.88 as compared to 141.0° for a cummingtonite with Fe/(Fe+Mg) = 0.38 (see table 6, Papike, Ross and Clark, 1969).

If the degree of tetrahedral rotation is a measure of strain resulting from the dimensional misfit between octahedral and tetrahedral layers, the presence of the smaller ferric ions would tend to reduce this misfit and alleviate the strain. This would explain the enhanced thermal stability limit of grunerite at moderately high oxygen fugacities. This argument is offered cautiously, as the equating of tetrahedral rotation to strain is somewhat tenous. Further, the magnitude of the strain may be trivial when compared to other factors controlling the thermal stability of the mineral. However, Hazen and Wones (1972) have shown that a governing factor in the stability of trioctahedral micas is the size of ions in octahedral coordination.

## GEOLOGICAL APPLICATIONS

The occurrence of grunerite is almost entirely restricted to moderately metamorphosed iron-rich sediments. The amphibole has been found in igneous rocks (Bowen and Schairer, 1935; Simonen and Vorma, 1969), but textural descriptions indicate it to be a deuteric alteration product, not a liquidus phase.

The occurrence of grunerite in the Biwabik Iron Formation, where it is the dominant constituent of metamorphosed slaty taconite, has been described by French (1968) and Bonnichsen (1969, 1975) among others. The iron formation has been intruded and thermally metamorphosed by the gabbros of the Duluth Complex. In the response of the iron-rich sediments to the metamorphic conditions, grunerite has proved to be an important index mineral. French (1968) has shown that four distinct metamorphic zones exist within the Biwabik Iron Formation as the contact with Duluth gabbro is approached. Zone 1 is the unaltered taconite consisting of quartz, magnetite, iron carbonates, and iron silicates such as minnesotaite. Zone 2 has the same mineralogy but is texturally distinct. Zone 3, the moderately metamorphosed taconite, is characterized by the appearance of grunerite and disappearance of the original taconite mineralogy. Within 3 km of the contact of the Duluth Complex, zone 4,

TABLE 3

| Grunerite annealed on MW buffer, 620°, 2kb | | | | |
|---|---|---|---|---|
| (hkl) | $2\theta$(calc) | $2\theta$(obs) | d(obs) | I |
| 020 | 9.58 | 9.55 | 9.26 | 10 |
| 110 | 10.59 | 10.50 | 8.41 | 100 |
| $11\bar{1}$ | 18.28 | 18.25 | 4.86 | <5 |
| 200* | 18.950 | 18.901 | 4.69 | 20 |
| 040* | 19.242 | 19.263 | 4.61 | 5 |
| 220* | 21.277 | 21.253 | 4.18 | 20 |
| $13\bar{1}$ | 22.84 | 22.90 | 3.88 | <5 |
| 131* | 25.641 | 25.646 | 3.47 | 5 |
| 240* | 27.134 | 27.139 | 3.28 | 35 |
| 060,310* | 29.036 | 28.982 | 3.08 | 100 |
| 221 | 29.74 | 29.70 | 3.00 | 5 |
| 151* | 32.257 | 32.247 | 2.77 | 30 |
| 061* | 33.315 | 33.861 | 2.64 | 10 |
| $20\bar{2}$ | 35.704 | 35.697 | 2.51 | 5 |
| 261 | 37.18 | 37.15 | 2.41 | <5 |
| 350 | 37.74 | 38.35 | 2.34 | <5 |
| $080,35\bar{1}$ | 39.054 | 39.018 | 2.30 | 10 |
| $31\bar{2}$* | 40.459 | 40.431 | 2.23 | 5 |
| $261,24\bar{2}$* | 40,837 | 40,874 | 2.20 | 15 |
| 081,202 | 42.86 | 42.90 | 2.10 | 5 |
| 351* | 44.177 | 44.171 | 2.05 | 5 |
| $51\bar{2}$ | 54.25 | 54.45 | 1.68 | <5 |
| 461* | 54.977 | 54.977 | 1.67 | 15 |
| 1 • 11 • 0 | 55.66 | 55.70 | 1.64 | 10 |
| 600 | 59.19 | 59.10 | 1.56 | 10 |
| 0 • 12 • 0 | 60.18 | 60.25 | 1.53 | 5 |
| $66\bar{1}$ | 66.219 | 66.246 | 1.41 | 15 |

a = 9.572(4)Å
b = 18.450(9)
c = 5.344(3)
$\beta$ = 101°55′(2)
V = 923(1)Å$^3$

* Reflections used for unit cell refinement.

the highly metamorphosed taconite is encountered. This zone is marked by the decomposition of grunerite to fayalite and/or orthopyroxenes and the conversion of carbonates to pyroxenes (French, 1968; Bonnichsen, 1975). Thus knowledge of the stability range of grunerite can provide data on the pressure-temperature conditions during the metamorphic event.

At the "grunerite isograd" of zone 3 (French, 1968), the amphibole forms from the original taconite minerals as the result of several reactions (see French, 1968, p. 81, for a description of possible reactions). Two reactions appear to be dominant, however: the breakdown of minnesotaite and the reaction of carbonates with quartz and water vapor. Forbes (1971a) has proposed temperatures of 270° to 300°C (1-2 kb $P_{(H_2O)}$) for the production of grunerite through the decomposition of minnesotaite. French (1973) suggests somewhat higher temperatures of 350° to 400°C for the formation of grunerite from siderite and chert. Of course, the temperatures of these reactions are strongly dependent on the magnesium

X-ray powder diffraction data for grunerite (Cu K$\alpha$ radiation)

| Grunerite oxidized in air | | | |
|---|---|---|---|
| 2$\theta$(calc) | 2$\theta$(obs) | d(obs) | I |
| 9.74 | 9.65 | 9.16 | 10 |
| 10.75 | 10.65 | 8.30 | 100 |
| 18.48 | Not observed | | |
| 19.228 | 19.187 | 4.62 | 20 |
| 19.567 | 19.774 | 4.48 | 10 |
| 21.60 | 21.55 | 4.12 | 5 |
| 23.14 | Not observed | | |
| 25.99 | 26.05 | 3.42 | 10B |
| 27.568 | 27.634 | 3.22 | 20 |
| 29.534 | 29.404 | 3.04 | 100 |
| 30.15 | Not observed | | |
| 32.745 | 32.893 | 2.73 | 25 |
| 34.343 | 34.410 | 2.61 | 10 |
| 36.098 | 36.049 | 2.49 | 15 |
| 37.76 | Not observed | | |
| 38.35 | Not observed | | |
| 39.646 | 39.624 | 2.27 | 10 |
| 40.94 | 40.90 | 2.20 | 5 |
| 41.479 | 41.383 | 2.18 | 10 |
| 43.56 | 43.50 | 2.07 | <5 |
| 44.86 | 44.80 | 2.02 | <5 |
| 55.00 | 54.90 | 1.67 | 5 |
| 55.86 | 55.90 | 1.64 | 10B |
| 56.68 | Not observed | | |
| 60.14 | 60.05 | 1.54 | 5 |
| 61.30 | Not observed | | |
| 67.318 | 67.330 | 1.39 | 10B |

a = 9.43(1)Å
b = 18.146(3)
c = 5.29(2)
$\beta$ = 101°59'(5)
V = 886(2)Å$^3$

content of participating phases, oxygen fugacity, and the fugacity of carbon dioxide.

At the higher grades of metamorphism, this study has shown that iron-rich grunerite will decompose in the temperature range 560° to 685°C (1kb, $P_{(H_2O)}$), depending on the values of oxygen fugacity existing during metamorphism. Within zone 4, Bonnichsen (1975) has found quartz, magnetite, and fayalite to be a fairly common assemblage throughout the iron formation. Thus, assuming that oxygen fugacity was close to that of the QFM buffer, the reaction of iron-rich grunerite with vapor to produce fayalite occurred at temperatures of 680° to 700°C with the assemblage fayalite, magnetite, quartz, and water vapor stable at temperatures greater than 700°C. This value is in excellent agreement with the temperature range suggested by Bonnichsen (1975) who estimates the metamorphic temperature maximum to be between 650° to 750°C at a total pressure of 1.5 to 3.0 kb.

## References


Bonnichsen, B., 1969, Metamorphic pyroxenes and amphiboles in the Biwabik Iron Formation, Dunka River, Minnesota: Mineralog. Soc. America Spec. Paper 2, p. 217-239.

———— 1975, Geology of the Biwabik Iron Formation, Dunka River Area, Minnesota: Econ. Geology, v. 70, p. 319-340.

Bowen, N. L., and Schairer, J. F., 1935, Grunerite from Rockport, Massachusetts, and a series of synthetic flour-amphiboles: Am. Mineralogist, v. 20, p. 543-551.

Boyd, F. R., 1959, Hydrothermal investigation of amphiboles, *in* Abelson, P. H., ed., Researches in geochemistry: New York, John Wiley & Sons, Inc., p. 377-396.

Charles, R. W., 1974, The physical properties of the Mg–Fe richterites: Am. Mineralogist, v. 59, p. 518-528.

Ernst, W. G., 1962, Synthesis, stability relations, and occurrence of riebeckite and riebeckite-arfuedsonite solid solutions: Jour. Geology, v. 70, p. 689-786.

———— 1968, Amphiboles: New York, Springer-Verlag, 125 p.

Eugster, H. P., 1957, Heterogeneous reactions involving oxidation and reduction at high pressures and temperatures: Jour. Chem. Physics, v. 26, p. 1760-1761.

Eugster, H. P., and Wones, D. R., 1962, Stability relations of the ferruginous biotite, anite: Jour. Petrology, v. 3, p. 82-125.

Evans, H. T., Appleman, D. E., and Handwerker, D. W., 1963, the Least squares refinement of crystal unit cells with powder diffraction data by an automatic computer indexing method [abs.]: Am. Cryst. Assoc., Ann Mtgs., Cambridge, Mass., Program, p. 42-43.

Finger, L. W., 1969, The crystal structure and cation distribution of a grunerite: Mineralog. Soc. America Spec. Paper 2, p. 95-100.

Flaschen, S. S., and Osborn, E. F., 1957, Studies in the system iron oxide–silica–water at low oxygen partial pressures: Econ. Geology, v. 52, p. 923-943.

Forbes, W. C., 1969, Unit cell parameters and optical properties of talc on the join $Mg_3Si_4O_{10}(OH)_2$–$Fe_3Si_4O_{10}(OH)_2$: Am. Mineralogist, v. 54, p. 1399-1408.

———— 1971a, Iron content of talc in the system $Mg_3Si_4O_{10}(OH)_2$–$Fe_3Si_4O_{10}(OH)_2$: Jour. Geology, v. 79, p. 63-74.

———— 1971b, Synthesis of grunerite, $Fe_7Si_8O_{22}(OH)_2$: Nature, v. 232, p. 109.

———— 1972, An interpretation of the hydroxyl contents of biotites and muscovites: Mineralog. Mag., v. 38, p. 712-720.

French, B. M., 1968, Progressive contact metamorphism of the Biwabik Iron Formation, Mesabi Range, Minnesota: Minnesota Geol. Survey Bull. 45, 102 p.

———— 1973, Mineral assemblages in diagenetic and low grade metamorphic iron-formation: Econ. Geology, v. 68, p. 1963-1974.

Gilbert, M. C., 1966, Synthesis and stability relationships of ferropargasite: Am. Jour. Sci., v. 264, p. 698-742.

Hazen, R. M., and Wones, D. R., 1972, The effect of cation substitutions on the physical properties of trioctahedral micas: Am. Mineralogist, v. 57, p. 103-129.

Huebner, J. S., and Sato, M., 1970, The oxygen fugacity—temperature relationships of manganese oxide and nickel oxide buffers: Am. Mineralogist, v. 55, p. 934-952.

James, H. L., 1955, Zones of regional metamorphism in the precambrian of Northern Michigan: Geol. Soc. America Bull., v. 66, p. 1455-1488.

Klein, C., Jr., 1964, Cummingtonite–grunerite series: a chemical, optical and X-ray study: Am. Mineralogist, v. 49, p. 963-000.

Kopp, O. C., and Harris, L. A., 1967, Synthesis of grunerite and other phases in the system $SiO_2$–NaOH–Fe–$H_2O$: Am. Mineralogist, v. 52, p. 1681-1688.

Mueller, R. F., 1960, Compositional characteristics and equilibrium relations in mineral assemblages of a metamorphosed iron formation: Am. Jour. Sci., v. 258, p. 449-497.

Papike, J. J., Ross, M., and Clark, J. R., 1969, Crystal-chemical characterization of clinoamphiboles based on five new structure refinements: Mineralog. Soc. America Spec. Paper 2, p. 117-135.

Schürmann, K., 1967, Hyorothermale experimentelle utersuchuncen an metamorphen monoklinen hornblenden. I. Zur stabilitat der cummingtonit: Neues Jahrb. Mineralogie Monatsh., v. 8, p. 270-284.

Semet, M. P., 1973, A crystal-chemical study of synthetic magnesio-hastingsite: Am. Mineralogist, v. 58, p. 480-494.

Sinonen, A., and Vorma, A., 1969, Amphibole and biotite from rapakivi: Comm. géol. Finlande Bull., no. 238, 28 p.

Tuttle, O. F., 1949, Two pressure vessels for silicate-water studies: Geol. Soc. America Bull., v. 60, p. 1727-1729.

Wones, D. R., 1963, Physical properties of synthetic biotites on the join phlogopite–annite: Am. Mineralogist, v. 48, p. 1300-1321.

Wones, D. R., and Gilbert, M. C., 1969, The fayalite–magnetite–quartz assemblage between 600° and 800°C: Am. Jour. Sci., v. 267A, p. 480-488.